European Journal of Medicinal Chemistry 45 (2010) 3087–3095

Contents lists available at ScienceDirect

European Journal of Medicinal Chemistry

journal homepage: http://www.elsevier.com/locate/ejmech

Original article

Synthesis of ruthenium(II) complexes and characterization of their cytotoxicity in vitro, apoptosis, DNA-binding and antioxidant activity

Yun-Jun Liu [a,*], Cheng-Hui Zeng [a], Zhen-Hua Liang [a], Jun-Hua Yao [b], Hong-Liang Huang [c,*], Zheng-Zheng Li [a], Fu-Hai Wu [d,*]

[a] School of Pharmacy, Guangdong Pharmaceutical University, Guangzhou, 510006, PR China
[b] Instrumentation Analysis and Research Center, Sun Yat-Sen University, Guangzhou, 510275, PR China
[c] School of Life Science and Biopharmacological, Guangdong Pharmaceutical University, Guangzhou, 510006, PR China
[d] School of Public Health, Guangdong Pharmaceutical University, Guangzhou, 510006, PR China

ARTICLE INFO

Article history:
Received 28 January 2010
Received in revised form
26 March 2010
Accepted 29 March 2010
Available online 3 April 2010

Keywords:
Ruthenium(II) complexes
DNA-binding
Cytotoxicity
Apoptosis

ABSTRACT

A new ligand DBHIP and its two ruthenium (II) complexes $[Ru(bpy)_2(DBHIP)](ClO_4)_2$ (**1**) and $[Ru(phen)_2(DBHIP)](ClO_4)_2$ (**2**) have been synthesized and characterized. The binding behaviors of the two complexes to calf thymus DNA were investigated by absorption spectra, viscosity measurements, thermal denaturation and photoactivated cleavage. The DNA-binding constants for complexes **1** and **2** have been determined to be $8.87 \pm 0.27 \times 10^4\ M^{-1}$ ($s = 1.83$) and $1.32 \pm 0.31 \times 10^5\ M^{-1}$ ($s = 1.84$). The results suggest that these complexes interact with DNA through intercalative mode. The cytotoxicity of DBHIP, complexes **1** and **2** has been evaluated by MTT assay. The apoptosis assay was carried out with acridine orange/ethidium bromide (AO/EB) staining methods. The studies on the mechanism of photocleavage demonstrate that superoxide anion radical ($O_2^{\cdot-}$) and singlet oxygen ($^1O_2$) may play an important role.

1. Introduction

Studies on the interaction of transition metal complexes with DNA continue to attract the attention of researcher due to their importance in design and development of synthetic restriction enzymes, chemotherapeutic drugs and DNA foot printing agents, DNA cleavage agents and DNA "molecular light switch" [1–7]. The interaction of DNA with ruthenium(II) polypyridine complexes containing planar polycyclic heteroaromatic ligand has been widely studied due to their unique spectroscopic and electrochemical properties [8–10]. The rich optical properties of these complexes facilitate assessments of their DNA-binding capabilities as binding to DNA can be probed through changes in absorption and emission spectra. Despite a considerable amount of literatures have reported that ruthenium(II) complexes can bind to DNA through intercalation [11–15]. The binding mode of parent $[Ru(phen)_3]^{2+}$ remains an issue of rigorous debate [16,17]. On the other hand, many Ru(II) polypyridyl complexes exert rather potent activities against selected tumor cells [18,19] and can be candidates for drugs. In this report, a new intercalative ligand DBHIP (2-(3,5-dibromo-4-hydroxyphenyl)imidazo[4,5-*f*][1,10]phenanthroline) and its Ru(II) complexes $[Ru(bpy)_2DBHIP](ClO_4)_2$ (**1**) (bpy = 2,2′-bipyridine) and $[Ru(phen)_2DBHIP](ClO_4)_2$ (**2**) (phen = 1,10-phenanthroline, Scheme 1) have been synthesized and characterized by elemental analysis, FAB-MS, ESI-MS, IR, ^1H NMR and ^{13}C NMR. The DNA-binding behaviors of these complexes were investigated by absorption titration, luminescence spectroscopy, thermal denaturation, viscosity measurements and photoactivated cleavage. The results show that complexes **1** and **2** interact with CT-DNA by intercalative mode. The studies on the mechanism of photocleavage reveal that singlet oxygen ($^1O_2$) and superoxide anion radical ($O_2^{\cdot-}$) may play an important role. The cytotoxicity of ligand DBHIP and complexes **1** and **2** has been evaluated by MTT assay. The apoptosis of BEL-7402 cells induced by Ru(II) complexes was investigated. The retardation assay of pGL 3 plasmid DNA by complexes **1** and **2** was also explored. The antioxidant activity of DBHIP and complexes **1** and **2** was performed by hydroxyl radical scavenging method.

2. Results and discussion

2.1. Synthesis and characterization

The ligand, DBHIP, was prepared with a method similar to that described by Steck and Day [20]. Refluxing of 1,10-phenanthroline-

Abbreviations: DBHIP, 2-(3,5-dibromo-4-hydroxyphenyl)imidazo[4,5-*f*][1,10]phenanthroline; CT-DNA, calf thymus; MTT, 3-(4,5-dimethylthiazol-2-yl)-2,5-diphenyltetrazolium bromide; bpy, 2,2′-bipyridine; phen, 1,10-phenanthroline.

* Corresponding author. Tel.: +86 20 39352122; fax: +86 20 39352128.
E-mail addresses: lyjche@163.com (Y.-J. Liu), hhongliang2004@yahoo.com.cn (H.-L. Huang), fuhaiwu@163.com (F.-H. Wu).

0223-5234/$ – see front matter Crown Copyright © 2010 Published by Elsevier Masson SAS. All rights reserved.
doi:10.1016/j.ejmech.2010.03.042

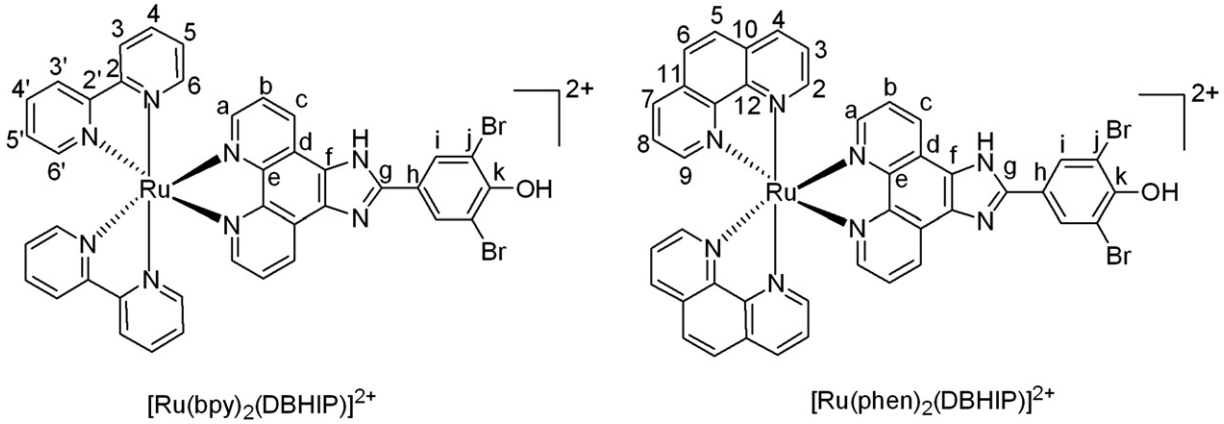

Scheme 1. The structure of complexes.

5,6-dione and 3,5-dibromo-4-hydroxybenzaldehyde in the presence of ammonium acetate and glacial acid produced the desired ligand in high yields. Complexes **1** and **2** were prepared by direct reaction of ligand with the appropriate mole ratios of the precursor complexes *cis*-$[Ru(bpy)_2Cl_2]\cdot 2H_2O$ [21] and *cis*-$[Ru(phen)_2Cl_2]\cdot 2H_2O$ [21] in ethanol. The yields were good to moderate. The desired Ru(II) complexes were isolated as their perchlorates and were purified by column chromatography. The structures of ligand and its complexes were confirmed by elemental analysis, FAB-MS, ES-MS, IR, ^{1}H NMR and ^{13}C NMR spectroscopy.

In the ^{1}H NMR spectra, for ligand and complexes **1** and **2**, the chemical shifts of protons on the nitrogen atoms of imidazole ring were not observed, probably because the protons are very active and easy to be exchanged quickly between the two nitrogens of the imidazole ring in solution, Similar examples have been reported previously [22]. The ^{13}C NMR sprectra for ligand and its complexes were assigned according to literature [23]. The changes of chemical shifts of C(a) of 3.58 and 2.86 ppm for complexes **1** and **2** in comparison with the free ligand are observed. This fact affirms that the free ligand is coordinated to metal. The complexes were also characterized by electrospray mass spectrometry (ESI-MS). In the ESI-MS spectra for the complexes **1** and **2**, as expected, the intense signals for $[M-2ClO_4-H]^+$ and $[M-2ClO_4]^{2+}$ were observed, the obtained molecular weights are consistent with the expected values.

2.2. DNA-binding studies

2.2.1. Electronic absorption titration

The electronic absorption spectra of complexes **1** and **2** mainly consist of three resolved bands. The low energy absorption band centered at 450–470 nm is assigned to metal-to-ligand charge transfer (MLCT) transition, the band at 330–350 nm is attributed to $\pi-\pi^*$ transition and the other band below 300 nm is attributed to intraligand (IL) $\pi-\pi^*$ transition by comparison with the spectrum of other polypyridyl Ru(II) complexes [13,24,25].

The absorption spectra of complexes **1** and **2** in the absence and presence of CT-DNA are given in Fig. 1. As the DNA concentration is increased, the MLCT transition bands of complexes **1** at 459 and **2** at 457 nm exhibit hypochromism of about 25.92 and 26.64%, and bathochromism of 2 and 3 nm, respectively, but the hypochromism at 337 nm for **1** and 343 nm for **2** reaches as high as 64.8 and 38.5%. These spectral characteristics may suggest a mode of binding that involves a stacking interaction between the aromatic chromophore and the DNA base pairs.

In order to further elucidate the binding strength of the complexes, the intrinsic constants K were determined by monitoring the changes of absorbance in the MLCT band with increasing concentration of CT-DNA. The values of K_b are $8.87 \pm 0.27 \times 10^4\ M^{-1}$ ($s = 1.83$) and $1.32 \pm 0.35 \times 10^5\ M^{-1}$ ($s = 1.84$) M^{-1} for **1** and **2**,

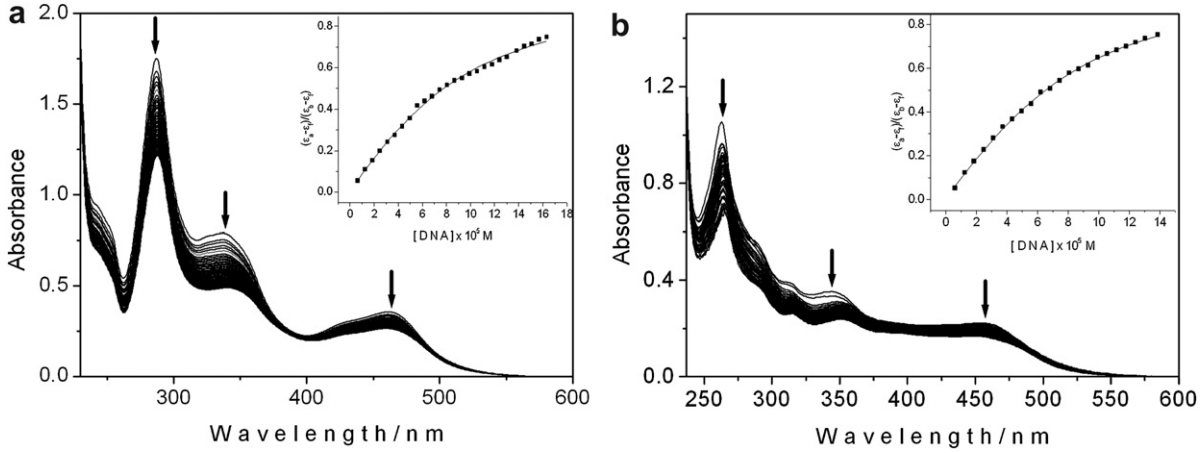

Fig. 1. Absorption spectra of complexes 1 (a) and 2 (b) in Tris–HCl buffer upon addition of CT-DNA. [Ru] = 20 μM. Arrow shows the absorbance change upon the increase of DNA concentration. Plots of $(\varepsilon_a - \varepsilon_f)/(\varepsilon_b - \varepsilon_f)$ *vs.* [DNA] for the titration of DNA with Ru(II) complexes.

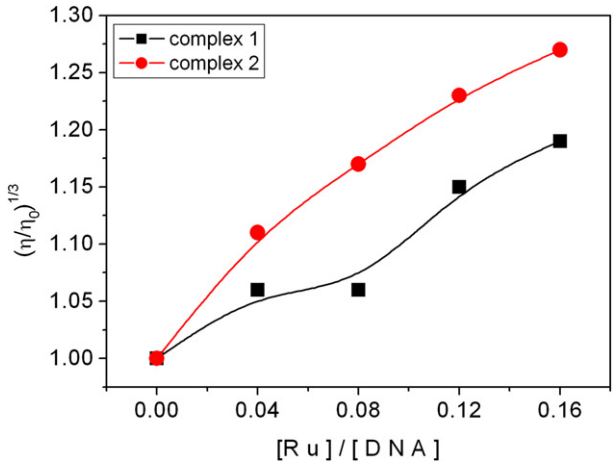

Fig. 2. Effect of increasing amounts of complexes 1 (■) and 2 (●) on the relative viscosity of calf thymus DNA at 25 (±0.1) °C. [DNA] = 0.30 mM.

respectively. These data suggest that the DNA-binding affinities of complexes are in the order: A(**2**) > A(**1**). These values are comparable to that of complexes $[Ru(bpy)_2PIP]^{2+}$ ($4.7 \pm 0.2 \times 10^5\ M^{-1}$, PIP = 2-phenylimidazo[4,5-*f*][1,10]phenanthroline) [26] and $[Ru(bpy)_2HPIP]^{2+}$ ($6.5 \pm 0.3 \times 10^5\ M^{-1}$, HPIP = 2-(2-hydroxyphenyl) imidazo[4,5-f][1,10]phenanthroline) [27] but is not as strong as that of $[Ru(bpy)_2dppz]^{2+}$ ($4.9 \times 10^6\ M^{-1}$, dppz = dipyrido[2,3-*a*:3′,2′-*c*] phenazine) [28].

2.2.2. Viscosity measurements

Further clarification of the interactions between the Ru(II) complexes and DNA was carried out by viscosity measurements. It is popularly accepted that a partial and/or nonclassical intercalation of ligand could bend (or kink) the DNA helix, reduces its effective length and, concomitantly, its viscosity; A classical intercalation of a ligand into DNA is known to cause a significant increase in the viscosity of a DNA solution due to an increase in the separation of the base pairs at the intercalation site and, hence, an increase in the overall DNA molecular length [29]. Fig. 2 shows the changes in the relative viscosity of CT-DNA on addition of **1** and **2**. Upon increasing the amounts of complexes **1** and **2**, the relative viscosity of CT-DNA solution increases steadily. These results suggest that complex **1** and **2** intercalates between the base pair of DNA.

2.2.3. Luminescence studies

Ruthenium(II) complexes can emit in the Tris buffer at room temperature. Emission intensity of complexes **1** and **2** from their MLCT excited states upon excitation at 459 and 457 nm is found to depend on DNA concentration. As shown in Fig. 3, upon the addition of CT-DNA, an obvious enhancement in emission intensity was observed for the two complexes. For complex **1** ($\lambda = 597$ nm), the emission intensity shows only around 126.33% increase and saturated at a [DNA]/[Ru] ratio of 7.44:1. For complex **2** ($\lambda = 589$ nm), the emission intensity shows around 161.45% increase saturated at a [DNA]/[Ru] ratio of 9.92:1. This clearly indicates that complex **2** is in a more hydrophobic environment in the presence of DNA when compared to complex **1**.

2.2.4. Thermal denaturation studies

The thermal behavior of DNA in the presence of complexes can give insight into the conformation change as the temperature is raised. The melting temperature T_m of DNA solution, which is defined as the temperature where half of the total base pairs is unbonded, is usually introduced to study the interaction of transition metal complexes with nucleic acid. Generally, the melting temperature of DNA increases when metal complexes bind to DNA by intercalation, as intercalation of the complexes between DNA base pairs causes stabilization of base stacking and hence raises the melting temperature of double-stranded DNA. The melting curves of CT-DNA in the absence and presence of complex are presented in Fig. 4. In the absence of any added complexes, the thermal denaturation carried out for DNA gave a T_m of 68.9 ± 0.2 °C under our experimental conditions. The melting point increased by +6.3 °C for complex **1** and +7.9 °C for complex **2**, respectively. The large increase in T_m of DNA with the two Ru(II) complexes are comparable to that observed for classical intercalators [30,31].

The binding constants of complexes **1** and **2** to CT-DNA at T_m were determined by McGee's equation [32].

$$\frac{1}{T_m^0} - \frac{1}{T_m} = \frac{R}{\Delta H_m}\ln(1 + KL)^{\frac{1}{n}} \quad (1)$$

where T_m^0 and T_m are the melting temperature of CT-DNA alone and in the presence of complex, respectively. ΔH_m is the enthalpy of DNA melting (per bp), R is the gas constant, K is the DNA-binding constant at T_m, L is the free Ru(II) complex concentration, and n is the binding site size.

The value of $\Delta H_m = 6.9$ kcal mol^{-1} was determined by different scanning calorimetry [29]. On the basis of the absorption spectra

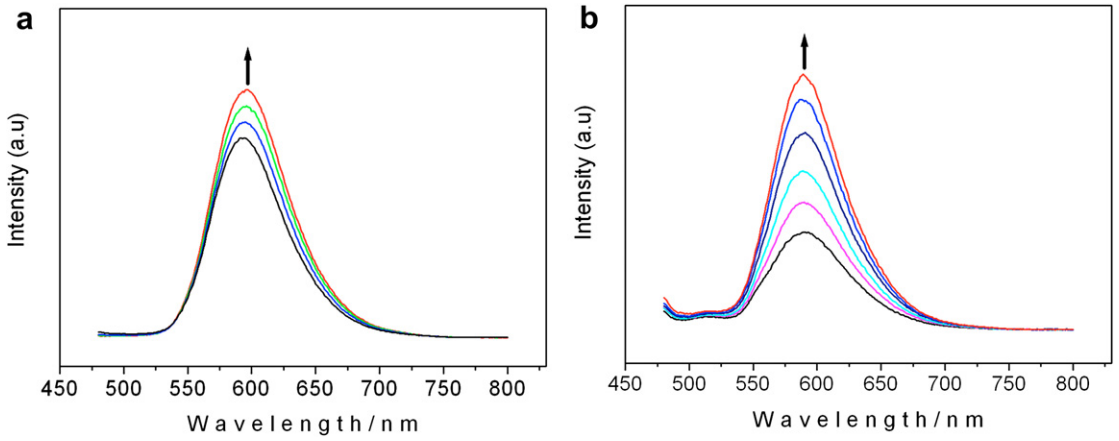

Fig. 3. Emission spectra of complexes 1 (a) and 2 (b) in Tris–HCl buffer in the absence and presence of CT-DNA. Arrow shows the intensity change upon increasing DNA concentrations.

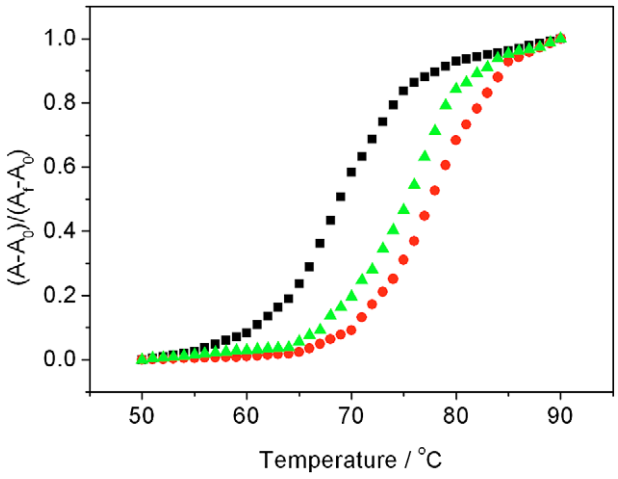

Fig. 4. Thermal denaturation of CT-DNA in the absence (■) and presence of complexes 1 (▲) and 2 (●). [Ru] = 32 μM, [DNA] = 80 μM.

titration experiment and the neighbor-exclusion principle, the values of *n* for complexes **1** and **2** were 1.83 and 1.84 bp (base pairs). The binding constants *K* for complexes **1** and **2** at T_m were calculated to be 2.31×10^3 and 3.45×10^3 M^{-1}, respectively. Comparing with those obtained from the absorption titration, although the binding constants obtained from thermal denaturation method are different from those obtained from absorption titration with the method suggested by Carter et al. [33], this difference between the two sets of binding constants should be caused by monitoring the absorption changes of different substances [DNA (260 nm), complexes **1** (459 nm) and **2** (457 nm)] and by different calculation method. According to the van't Hoffs equations (2–4) [34]

$$\ln\left(\frac{K_2}{K_1}\right) = \frac{\Delta H^0}{R}\left(\frac{1}{T_1} - \frac{1}{T_2}\right) \quad (2)$$

$$\Delta G_T^0 = -RT\ln K \quad (3)$$

$$\Delta G_T^0 = \Delta H - T\Delta S^0 \quad (4)$$

where K_1 and K_2 are the DNA-binding constants of the complexes at the temperature of T_1 and T_2, respectively. ΔH^0, ΔG_T^0 and ΔS^0 are the changes of standard enthalpy, standard free energy and standard entropy of binding of the complex to CT-DNA. The values of ΔG_T^0, ΔH^0, and ΔS^0 were -28.23 kJ mol^{-1}, -62.72 kJ mol^{-1} and -115.77 J mol^{-1} K^{-1} for complex **1**, and -29.21 kJ mol^{-1}, -60.99 kJ mol^{-1} and -106.64 J mol^{-1} K^{-1} for complex **2**.

2.2.5. Photoactivated cleavage of pBR 322 DNA

When circular plasmid DNA is subject to electrophoresis, relatively fast migration will be observed for the intact supercoiled form (Form I); If scission occurs on one strand (nicked), the supercoiled will relax to generate a slower-moving open circular form (Form II) [35]. A number of metal polypyridyl complexes have been shown to exhibit DNA photocleaving ability [6,13,15]. The

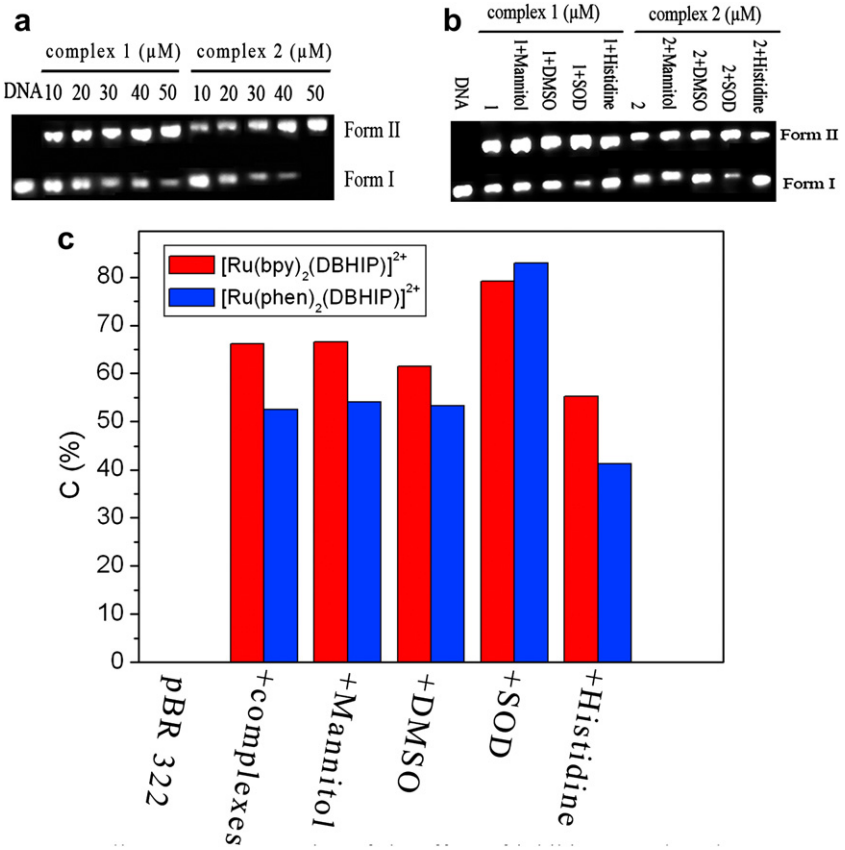

Fig. 5. (a) Photoactivated cleavage of pBR 322 DNA in the presence of different concentrations of Ru(II) complexes after irradiation at 365 nm for 30 min. (b) Photoactivated cleavage of supercoiled pBR 322 DNA by complex 1 and 2 (20 μM) in the absence and presence of different inhibitors [100 mM mannitol, 200 mM dimethylsulfoxide (DMSO), 1000 U ml^{-1} superoxide dismutase (SOD), 1.2 mM distidine] after irradiation at 365 nm for 30 min. (c) Bar diagram representation of the effect of inhibitors on the photoactivated cleavage activity of complexes **1** and **2**.

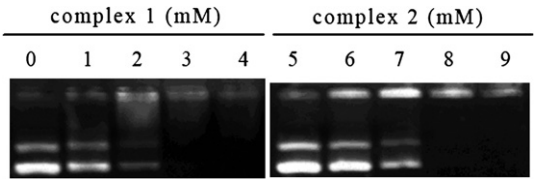

Fig. 6. Agarose gel electrophoresis retardation of pGL 3 plasmid DNA by complexes 1 and 2. Lane (0, 5) (DNA alone), lane 1–4, 6–9 in the different concentration of Ru(II) complexes. **1**: (1) 0.33 mM; (2) 1 mM; (3) 1.67 mM; (4) 2.33 mM. **2**: (6) 0.33 mM; (7) 1 mM; (8) 1.67 mM; (9) 2.33 mM. [DNA] = 0.5 μg.

cleavage of plasmid DNA can be monitored by agarose gel electrophoresis. As shown in Fig. 5a, both complexes are able to photocleave pBR 322 DNA. No obvious DNA cleavage was observed for the control in which metal complex was absent (DNA alone), or incubation of the plasmid with the Ru(II) complexes in the dark (data not presented). With increasing concentration of complexes, the Form I decrease and Form II increase gradually. Under the same experimental condition, complex **2** exhibits more effective DNA cleavage activity than complex **1**. The different cleaving efficiency may be ascribed to the different binding affinity of two Ru(II) complexes to DNA.

In order establish the reactive species responsible for the photoactivated cleavage of the plasmid, the influence of different potentially inhibiting agents was investigated. Fig. 5b shows that the DNA cleavage of the plasmid by complexes **1** and **2** was not inhibited in the presence of hydroxyl radical (OH•) scavengers such as mannitol [36] and dimethylsulfoxide (DMSO) [37], which indicated that hydroxyl radical was not likely to be the cleaving agent. In the presence of superoxide dismutase (SOD), a facile superoxide anion radical ($O_2^{\bullet-}$) quencher, the cleavage was obviously improved. The DNA cleavage of the plasmid was inhibited in the presence of the singlet oxygen ($^1O_2$) scavenger histidine [38], suggesting that $^1O_2$ is likely to be the reactive species responsible for the cleavage reaction. Related results of enhancement by SOD and inhibition by singlet oxygen scavengers have been observed by other ruthenium intercalators [6,13,23]. Fig. 5c shows the bar diagram representation of the percentage of cleavage (C) for complexes **1** and **2**.

2.2.6. Retardation of pGL 3 plasmid DNA by Ru(II) complexes

DNA condensation into compact structures has been received considerable attention to understand the mechanism of uptake of gene vectors in living cells. Several studies reported the polyamine can condense DNA [39–41]. However, the studies of small molecules to condense DNA have been less paid attention. Ji and co-workers reported the Ru(II) complexes $[Ru(bpy)_2(PIPSH)]^{2+}$ and $[Ru(phen)_2(PIPSH)]^{2+}$ [42] can effectively condense DNA at a concentration of 80 μM. The abilities of complexes **1** and **2** to condense pGL 3 DNA were evaluated by gel retardation assay. Fig. 6 shows when the concentrations of complexes **1** and **2** are 0.33 and 1.0 mM, complex **1** and **2** cannot condense the DNA, however, the concentrations of **1** and **2** reach 1.67 and 2.33 mM, the effects of condensation of DNA were observed.

2.3. Cytotoxic assay in vitro

Research on bioactive polypyridyl complexes is a very active field and has been paid great attention. Many polypyridyl complexes show interesting bioactivity, complex $[Ru(bpy)_2(dppn)]^{2+}$ can effectively inhibit the proliferation of MCF-7 cells with a low IC_{50} (3.3 ± 1.2 μM)

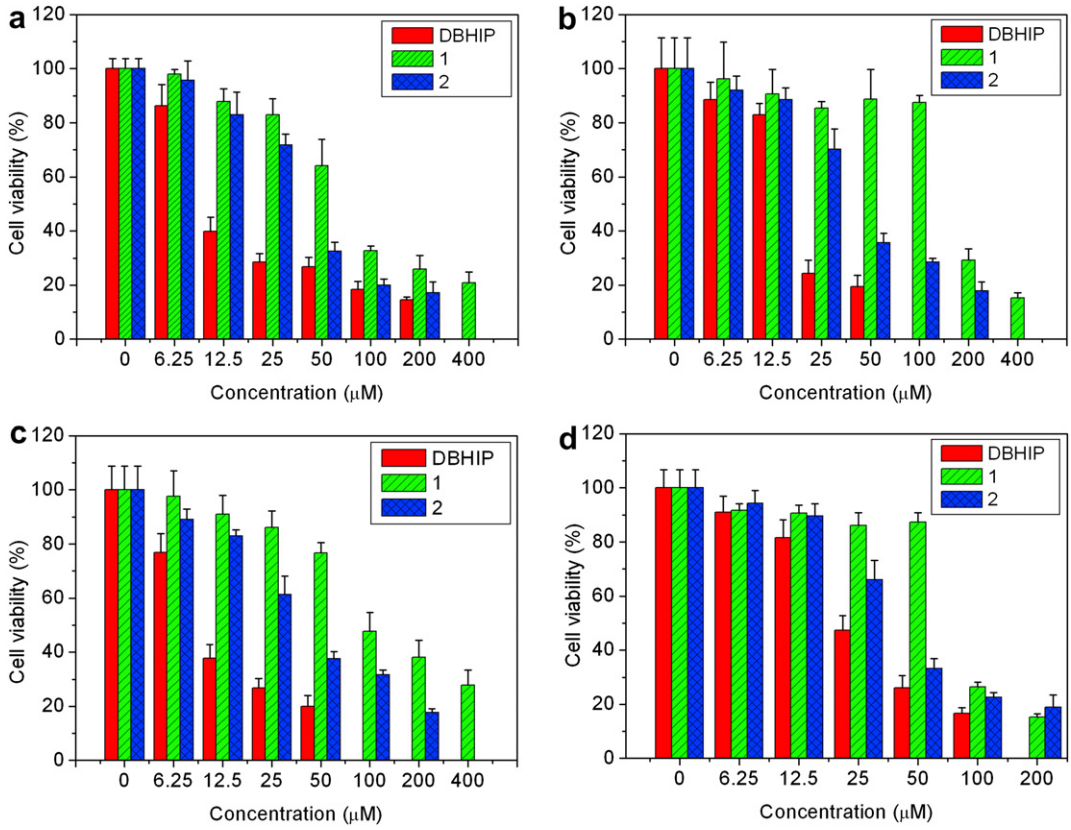

Fig. 7. Cell viability of DBHIP, 1 and 2 on tumor BEL-7402 (a), C-6 (b), HepG-2 (c) and MCF-7 (d) cell proliferation in vitro. Each data point is the mean ± standard error obtained from three independent experiments.

Table 1
The IC_{50} values for DBHIP, complexes **1** and **2** against selected cell lines.

Compound	IC_{50} (μM)				
	BEL-7402(24 h)	BEL-7402 (48 h)	C-6	HepG-2	MCF-7
DBHIP	15.26 ± 4.11	11.18 ± 3.87	15.05 ± 4.45	10.65 ± 3.62	18.45 ± 2.89
1	56.10 ± 4.59	41.29 ± 4.58	>100	>100	>100
2	33.18 ± 3.59	21.62 ± 3.71	30.75 ± 3.50	28.35 ± 2.58	21.91 ± 2.52
cis-Platin	30.25 ± 3.64	20.12 ± 2.35	10.26 ± 2.78	26.25 ± 3.12	11.34 ± 2.38

[43]. Treatment of HT-29 and MCF-7 cells with [Rh(DMSO)Cl_3(dpq)] leads to significant decreases in cellular oxygen consumption and the rate of extracellular acidification [44]. To test the cytoxicity of ligand and ruthenium(II) complexes, BEL-7402 (hepatocellular), C-6 (Rat glioma), HepG-2 (hepatocellular) and MCF-7 (breast cancer) cell lines were cultured in the presence of varying concentrations of ligand and corresponding ruthenium(II) complexes for 48 h. The cytoxicity was analyzed by MTT assay as described in the experimental section. The inhibitory concentration 50 (IC_{50}), defined as the concentration required to reduce the size of the cell population by 50%. The IC_{50} values obtained of ligand and its complexes against selected four tumor cell lines are given in Table 1. The cell viability (%) obtained with continuous exposure for 48 h are depicted in Fig. 7. The toxicity of ligand and complexes was found to be concentration dependent, the cell viability decreased with increasing the concentration of DBHIP, **1** and **2**. The IC_{50} values are 11.18, 15.06, 10.65, 18.45 for DBHIP, 41.29, >100, >100, >100 for complex **1**, and 21.62, 30.75, 28.35, 21.91 for complex **2** against BEL-7402, C-6, HepG-2 and MCF-7 cell lines, respectively. Comparing the IC_{50} values of complexes **1** and **2**, complex **2** appeared to be higher cytotoxicity than complex **1**, but smaller than those of cisplatin. Furthermore, we also found that the coordination of the DBHIP to the Ru(II) metal center to form complexes **1** and **2**, the antitumor activity of DBHIP was obviously weakened.

2.4. Apoptosis assay

Induction of apoptosis is one of the considerations in drug development, most of the cytotoxic anticancers drugs in current use have been shown to induce apoptosis in susceptible cells [45]. On the basis of overall cell morphology and cell membrane integrity, necrotic and apoptotic cells can be distinguished from one another using fluorescence microscope. Fluorescence microscopic analysis showed untreated BEL-7402 cells were stained with uniform green fluorescence (Fig. 8a). After treatment with complex **2** for a period of 24 h, the clear morphological changes in the nucleolus was observed (Fig. 8b) and green apoptotic cells containing apoptotic bodies, as well as red necrotic cells, were also found. Similar result was also observed for complex **1**.

2.5. Antioxidant activity

The hydroxyl radical (OH•) in aqueous media was generated by the Fenton system [46]. The antioxidant activity of the ligand DBHIP and complexes **1** and **2** against hydroxyl radical (OH•) were investigated. Fig. 9 and Table 2 depict the inhibitory effect of ligand and complexes on OH•. The average suppression ratios for OH• increase with the increasing concentration of DBHIP, **1** and **2** in the range of 0.5–3.5 μM. The suppression ratio against OH• valued from 1.05 to 52.92% for DBHIP, 7.62 to 68.76% for complex **1** and 6.88 to 61.73% for complex **2**. The antioxidant activity against hydroxyl radical of complexes **1** (IC_{50} = 0.70 μM) and **2** (IC_{50} = 0.80 μM) is comparable under the same experimental condition. It is clear that the hydroxyl radical scavenging activity can be enhanced when ligand (IC_{50} = 1.11 μM)

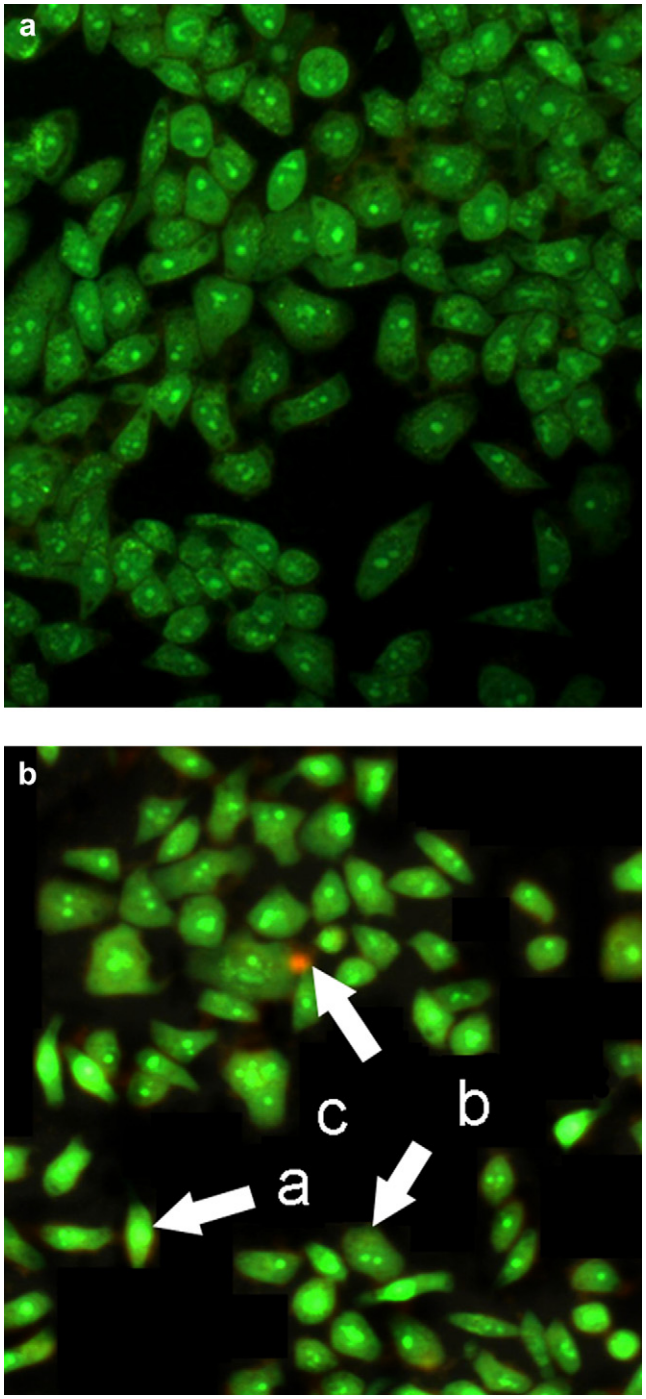

Fig. 8. BEL-7402 cell were stained by AO/EB and observed under fluorescence microscopy. BEL-7402 cell without treatment (a) and in the presence of complex **2** (b) incubated at 37 °C and 5% CO_2 for 24 h. Cells in a, b and c are apoptotic, living and necrotic cells, respectively.

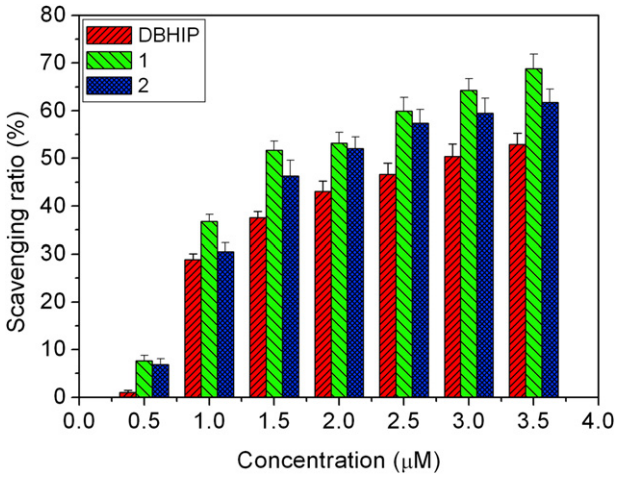

Fig. 9. Scavenging effect of the ligand DBHIP and complexes **1** and **2** on hydroxyl radicals. Experiments were performed in triplicate.

bonds Ru(II) metal center to form complexes. Similar results were also observed for other ruthenium(II) complexes [22]. Due to the lower IC_{50} values, DBHIP and complexes **1** and **2** may be potential drugs to eliminate the radicals.

3. Conclusion

A new ligand DBHIP and its two ruthenium(II) complexes $[Ru(bpy)_2(DBHIP)]^{2+}$ and $[Ru(phen)_2(DBHIP)]^{2+}$ have been synthesized and characterized. The DNA-binding of these complexes with CT-DNA indicates that the two complexes can intercalate between DNA base pairs via intercalative ligand DBHIP. When irradiated at 365 nm, complexes **1** and **2** can efficiently cleave the plasmid pBR 322 DNA. The mechanism studies of photoactivated cleavage reveal that singlet oxygen ($^1O_2$) and superoxide anion radical ($O_2^{\bullet-}$) may play an important role in the photocleavage. Cytotoxicity evaluation in vitro shows that the ligand and its complex **2** all displayed antitumor activity against the selected tumor cell lines and complexes **1** and **2** can induce the apoptosis of BEL-7402 cells. At high concentration, complexes **1** and **2** can effectively condense pGL 3 plasmid DNA. The experiments on antioxidant activity show that ligand and its complexes may be potential drugs to eliminate the radicals.

4. Experimental

4.1. Materials and methods

Calf thymus DNA (CT-DNA) was obtained from the Sino-American Biotechnology Company. pBR 322 DNA was obtained from Shanghai Sangon Biological Engineering & Services Co., Ltd. Dimethylsulfoxide (DMSO) and RPMI 1640 were purchased from Sigma. Cell lines of BEL-7402 (hepatocellular), C-6 (Rat glioma), HepG-2 (hepatocellular) and MCF-7 (breast cancer) were purchased from American Type Culture Collection, agarose and ethidium bromide were obtained from Aldrich. $RuCl_3 \cdot xH_2O$ was purchased from Kunming Istitution of Precious Metals. 1,10-phenanthroline was obtained from Guangzhou Chemical Reageng Factory. Doubly distilled water was used to prepare buffers (5 mM Tris(hydroxymethylaminomethane)–HCl, 50 mM NaCl, pH = 7.2). A solution of calf thymus DNA in the buffer gave a ratio of UV absorbance at 260 and 280 nm of ca. 1.8–1.9:1, indicating that the DNA was sufficiently free of protein [47]. The DNA concentration per nucleotide was determined by absorption spectroscopy using the molar absorption coefficient (6600 M^{-1} cm^{-1}) at 260 nm [48].

Microanalysis (C, H, and N) was carried out with a Perkin–Elmer 240Q elemental analyzer. Fast atom bombardment (FAB) mass spectra were recorded on a VG ZAB-HS spectrometer in a 3-nitrobenzyl alcohol matrix. Electrospray mass spectra (ES-MS) were recorded on a LCQ system (Finnigan MAT, USA) using methanol as mobile phase. The spray voltage, tube lens offset, capillary voltage and capillary temperature were set at 4.50 kV, 30.00 V, 23.00 V and 200 °C, respectively, and the quoted *m/z* values are for the major peaks in the isotope distribution. ^1H NMR and ^{13}C NMRR spectra were recorded on a Varian-500 spectrometer. All chemical shifts were given relative to tetramethylsilane (TMS). UV/Vis spectra were recorded on a Shimadzu UV-3101PC spectrophotometer at room temperature.

4.2. Synthesis of ligand and complexes

4.2.1. Synthesis of ligand (DBHIP)

A mixture of 1,10-phenanthroline-5,6-dione (0.315 g, 1.5 mmol), 3,5-dibromo-4-hydroxyphenylaldehyde (0.419 g, 1.5 mmol), ammonium acetate (2.31 g, 30 mmol) and glacial acetic acid (30 cm^3) was refluxed with stirring for 2 h. The cooled solution was diluted with water and neutralized with concentrated aqueous ammonia. The precipitate was collected and purified by column chromatography on silica gel (60–100 mesh) with ethanol as eluent to give the compound as yellow powder. Yield: 81%. Anal. Calcd. for $C_{19}H_{10}N_4Br_2O$: C, 48.54; H, 2.14; N, 11.92; Found: C, 48.51; H, 2.18; N, 11.89%. FAB-MS: $m/z = 471$ $[M+1]^+$. IR (KBr, cm^{-1}): 3437, 2927, 1604, 1589, 1476, 1449, 1357, 1173, 1109, 1073, 805, 736, 670. ^1H NMR (500 MHz, DMSO-d_6): 9.02 (d, 2H, H_c, $J = 8.5$ Hz), 8.33 (d, 2H, H_i, $J = 8.4$ Hz), 8.01 (d, 2H, H_a, $J = 8.6$ Hz), 7.22 (d, 2H, H_b, $J = 8.2$ Hz), 3.26 (s, 1H, H_{O-H}). ^{13}C NMR (DMSO-d_6, ppm): 163.35 C(k), 151.79 C(a), 147.02 C(c), 142.46 C(g), 129.75 C(h), 129.29 C(d, e, f), 123.08 C(i), 114.94 C(b), 109.71 C(j).

4.2.2. Synthesis of $[Ru(bpy)_2(DBHIP)](ClO_4)_2$ (**1**)

A mixture of *cis*-$[Ru(bpy)_2Cl_2] \cdot 2H_2O$ (0.260 g, 0.5 mmol) and DBHIP (0.185 g, 0.5 mmol) in ethanol (30 cm^3) was refluxed under argon for 8 h to give a clear red solution. Upon cooling, a red precipitate was obtained by dropwise addition of saturated aqueous $NaClO_4$ solution. The crude product was purified by column chromatography on a neutral alumina with a mixture of CH_3CN-toluene (3:1, v/v) as eluant. The mainly red band was collected. The solvent

Table 2
The influence of investigated compounds for $OH^{\bullet}$.

Comp	Average inhibition (%) for OH (μM)							Equation	IC_{50} (μM)	R^2
	0.5	1.0	1.5	2.0	2.5	3.0	3.5			
DBHIP	1.05	28.85	37.52	43.05	46.64	50.37	52.92	$Y = 47.20+58.92x$	1.12	0.9804
1	7.62	36.77	51.72	53.21	59.94	64.27	68.76	$Y = 60.69+69.26x$	0.70	0.9837
2	6.88	30.49	46.34	52.02	57.40	59.49	61.73	$Y = 56.09+65.81x$	0.81	0.9871

IC_{50} values were calculated from regression lines where: x was log of the tested compound concentration and Y was percent inhibition of the tested compounds. When the percent inhibition of the tested compounds was 50%, the tested compound concentration was IC_{50}. R^2 = correlation coefficient.

was removed under reduced pressure and a red powder was obtained. Yield: 73%. Anal. Calcd. for $C_{39}H_{26}Br_2Cl_2N_8O_9Ru$: C, 43.27; H, 2.42; N, 10.35; found: C, 43.23; H, 2.47; N, 10.37%. ESI-MS [CH_3CN, m/z]: 883.1 ([M−2ClO_4−H]$^+$), 442.3 ([M−2ClO_4]$^{2+}$). IR (KBr, cm^{-1}): 3433, 2923, 1602, 1584, 1445, 1423, 1363, 1121, 1088, 804, 767, 731, 670. ^{1}H NMR (500 MHz, DMSO-d_6): δ 9.04 (d, 2H, H_c, $J = 8.0$ Hz), 8.88 (d, 2H, H_3, $J = 8.5$ Hz), 8.84 (d, 2H, $H_{3'}$, $J = 8.0$ Hz), 8.22 (dd, 4H, $H_{4,4'}$, $J = 7.8$ Hz), 8.08 (d, 2H, H_i, $J = 8.0$ Hz), 7.91 (d, 2H, H_a, $J = 8.0$ Hz), 7.80 (d, 2H, H_6, $J = 8.0$ Hz), 7.78 (dd, 2H, $H_{6'}$, $J = 7.6$ Hz), 7.58 (ddd, 4H, $H_{5,5'}$), 7.35 (dd, 2H, H_b, $J = 7.7$ Hz), 3.37 (s, 1H, H_{O-H}). ^{13}C NMR (DMSO-d_6, ppm): 164.56 C (k), 156.81 C(2), 156.55 C(2′), 151.33 C (6, 6′), 148.21 C(a), 143.75 C(c, g), 137.78 C(4), 137.61 C(4′), 130.20 C(d, e, f), 129.74 C(h), 127.79 C(3), 127.71 C(3′), 125.41 C(i, b), 124.39 C(5), 124.32 C(5′), 115.09 C(j).

4.2.3. Synthesis of [Ru(phen)$_2$(DBHIP)](ClO$_4$)$_2$ (**2**)

This complex was synthesized in an manner identical to that described for complex **1**, with *cis*-[Ru(phen)$_2$Cl$_2$]·2H$_2$O (0.280 g, 0.5 mmol) in place of *cis*-[Ru(bpy)$_2$Cl$_2$]·2H$_2$O. Yield: 72%. Anal. Calcd. for $C_{43}H_{26}Br_2Cl_2N_8O_9Ru$: C, 45.68; H, 2.32; N, 9.91; Found: C, 45.64; H, 2.34; N, 9.95%. ESI-MS [CH_3CN, m/z]: 930.0 ([M−2ClO_4−H]$^+$), 465.53 ([M−2ClO_4]$^{2+}$). IR (KBr, cm^{-1}): 3411, 2934, 1601, 1583, 1443, 1425, 1366, 1196, 1144, 1087, 845, 721, 626. ^{1}H NMR (500 MHz, DMSO-d_6): δ 9.02 (d, 2H, H_c, $J = 8.4$ Hz), 8.767 (d, 4H, $H_{4,7}$, $J = 8.5$ Hz), 8.39 (s, 4H, $H_{5,6}$), 8.29 (s, 2H, H_i), 8.13 (d, 2H, H_a, $J = 8.4$ Hz), 8.08 (d, 2H, H_2, $J = 8.0$ Hz), 7.96 (d, 2H, H_9, $J = 8.2$ Hz), 7.74–7.79 (m, 6H, $H_{3,8,b}$), 3.37 (s, 1H, H_{O-H}). ^{13}C NMR (DMSO-d_6, ppm): 163.42 C(k), 152.65 C(2), 152.55 C(9), 148.93 C(a), 147.25 C(4), 147.17 C(7), 144.24 C (c, g), 136.63 C(h, 12), 130.36 C(5), 130.15 C(6), 129.65 C(d, e, f, 10, 11), 128.01 C(3), 127.97 C(8), 126.23 C(i), 125.38 C(b), 115.00 C(j).

Caution: Perchlorate salts of metal compounds with organic ligands are potentially explosive, and only small amounts of the material should be prepared and handled with great care.

4.3. DNA-binding and photoactivated cleavage

The DNA-binding and photoactivated cleavage experiments were performed at room temperature. Buffer A [5 mM tris (hydroxymethyl)aminomethane (Tris) hydrochloride, 50 mM NaCl, pH 7.0] was used for absorption titration, luminescence titration and viscosity measurements. Buffer B (50 mM Tris–HCl, 18 mM NaCl, pH 7.2) was used for DNA photocleavage experiments. Buffer C (1.5 mM Na_2HPO_4, 0.5 mM NaH_2PO_4, 0.25 mM Na_2EDTA, pH 7.0) was used for thermal DNA denaturation experiments. Buffer D (0.9% of physiological saline) was used for retardation assay of pGL 3 plasmid DNA.

The absorption titrations of the complex in buffer were performed using a fixed concentration (20 μM) for complex to which increments of the DNA stock solution were added. Ru-DNA solutions were allowed to incubate for 5 min before the absorption spectra were recorded. The intrinsic binding constants K, based on the absorption titration, were measured by monitoring the changes of absorption in the MLCT band with increasing concentration of DNA using the following equation [33].

$$\frac{\varepsilon_a - \varepsilon_f}{\varepsilon_b - \varepsilon_f} = \frac{\sqrt{b - \left(b^2 - 2K^2C_t[\mathrm{DNA}]/s\right)}}{2KC} \tag{5a}$$

$$b = 1 + KC_t + K[\mathrm{DNA}]/2s \tag{5b}$$

where [DNA] is the concentration of CT-DNA in base pairs, the apparent absorption coefficients ε_a, ε_f and ε_b correspond to A_{obsed}/[Ru], the absorbance for the free ruthenium complex, and the absorbance for the ruthenium complex in fully bound form, respectively. K is the equilibrium binding constant, C_t is the total metal complex concentration in nucleotides and s is the binding site size.

Thermal denaturation studies were carried out with a Perkin-Elmer Lambda 35 spectrophotometer equipped with a Peltier temperature-controlling programmer (± 0.1 °C). The melting temperature (T_m) was taken as the mid-point of the hyperchromic transition. The melting curves were obtained by measuring the absorbance at 260 nm for solutions of CT-DNA (80 μM) in the absence and presence of the Ru(II) complex (32 μM) as a function of the temperature. The temperature was scanned from 50 to 90 °C at a speed of 1 °C min^{-1}. The data were presented as $(A - A_0)/(A_f - A_0)$ versus temperature, where A, A_0, and A_f are the observed, the initial, and the final absorbance at 260 nm, respectively.

Viscosity measurements were carried out using an Ubbelodhe viscometer maintained at a constant temperature at 25.0 (±0.1) °C in a thermostatic bath. DNA samples approximately 200 base pairs in average length were prepared by sonicating in order to minimize complexities arising from DNA flexibility [49]. Flow time was measured with a digital stopwatch, and each sample was measured three times, and an average flow time was calculated. Relative viscosities for DNA in the presence and absence of complexes were calculated from the relation $\eta = (t - t^0)/t^0$, where t is the observed flow time of the DNA-containing solution and t^0 is the flow time of buffer alone [28,50]. Data were presented as $(\eta/\eta_0)^{1/3}$ versus binding ratio [51], where η is the viscosity of DNA in the presence of complexes and η_0 is the viscosity of DNA alone.

For the gel electrophoresis experiment, supercoiled pBR 322 DNA (0.1 μg) was treated with the Ru(II) complexes in buffer B, and the solution was then irradiated at room temperature with a UV lamp (365 nm, 10 W). The samples were analyzed by electrophoresis for 1.5 h at 80 V on a 0.8% agarose gel in TBE (89 mM Tris–borate acid, 2 mM EDTA, pH = 8.3). The gel was stained with 1 μg/ml ethidium bromide and photographed on an Alpha Innotech IS-5500 fluorescence chemiluminescence and visible imaging system. The integrated density values (IDV) were given by FluorChem 5500 software. The percentage of cleavage (C) was calculated according to Eq. (6), where D_I, D_{II} and D_{III} are the IDVs of Form I (supercoil form), Form II (nicking form) and Form III (linear form), respectively.

$$C = \frac{D_{II} + 2D_{III}}{D_I + D_{II} + D_{III}} \tag{6}$$

4.4. Cytotoxicity assay

Standard 3-(4,5-dimethylthiazole)-2,5-diphenyltetraazolium bromide (MTT) assay procedures were used [52]. Cells were placed in 96-well microassay culture plates (1×10^4 cells per well) and grown overnight at 37 °C in a 5% CO_2 incubator. Test compounds were then added to the wells to achieve final concentrations ranging from 10^{-6} to 10^{-4} M. Control wells were prepared by addition of culture medium (100 μL). Wells containing culture medium without cells were used as blanks. The plates were incubated at 37 °C in a 5% CO_2 incubator for 48 h. Upon completion of the incubation, stock MTT dye solution (20 μL, 5 mg mL^{-1}) was added to each well. After 4 h incubation, buffer (100 μL) containing *N*,*N*-dimethylformamide (50%) and sodium dodecyl sulfate (20%) was added to solubilize the MTT formazan. The optical density of each well was then measured on a microplate spectrophotometer at a wavelength of 490 nm. The IC_{50} values were determined by plotting the percentage viability versus concentration on a logarithmic graph and reading off the concentration at which 50% of cells remain viable relative to the control. Each experiment was repeated at least three times to get the mean values. Four different

tumor cell lines were the subjects of this study: BEL-7402 (hepatocellular), C-6 (Rat glioma), HepG-2 (hepatocellular) and MCF-7 (breast cancer) (purchased from American Type Culture Collection).

4.5. Apoptosis studies

Apoptosis studies were performed with a staining method utilizing acridine orange (AO) and ethidium bromide (EB) [53]. According to the difference in membrane integrity between necrotic and apoptosis. AO can pass through cell membrane, but EB cannot. Under fluorescence microscope, live cells appear green. Necrotic cells stain red but have a nuclear morphology resembling that of viable cells. Apoptosis cells appear green, and morphological changes such as cell blebbing and formation of apoptotic bodies will be observed.

A monolayer of BEL-7402 cells was incubated in the absence and presence of complex **2** at concentration of 25 μM at 37 °C and 5% CO_2 for 24 h. After 24 h, each cell culture was stained with AO/EB solution (100 μg ml^{-1} AO, 100 μg ml^{-1} EB). Samples were observed under a fluorescence microscope.

4.6. Scavenger measurements of hydroxyl radical (OH•)

The hydroxyl radical (OH•) in aqueous media was generated by the Fenton system [46]. The solution of the tested complexes was prepared with DMF (N,N-dimethylformamide). The 4 ml of assay mixture contained following reagents: safranin (28.5 μM), EDTA-Fe (II) (100 μM), H_2O_2 (44.0 μM), the tested compounds (0.5–3.5 μM) and a phosphate buffer (67 mM, pH = 7.4). The assay mixtures were incubated at 37 °C for 30 min in a water bath. After which, the absorbance was measured at 520 nm. All the tests were run in triplicate and expressed as the mean. A_i was the absorbance in the presence of the tested compound; A_0 was the absorbance in the absence of tested compounds; A_c was the absorbance in the absence of tested compound, EDTA-Fe(II), H_2O_2. The suppression ratio (η_a) was calculated on the basis of $(A_i - A_0)/(A_c - A_0) \times 100\%$.

Acknowledgements

This research is supported by the National Nature Science Foundation of China (No. 30800227), the Science and Technology Foundation of Guangdong Province (No. 2009B030803057) and GuangdongPharmaceutical University for financial supports.

References

[1] A. Sigel, H. Sigel. (eds.), vol. 33, Marcel Dekker, New York (1996) pp. 177–252.
[2] L.N. Ji, X.H. Zou, J.G. Liu, Coord. Chem. Rev. 216–217 (2001) 513–536.
[3] V.G. Vaidyananthan, B.H. Nair, Dalton Trans. (2005) 2842–2848.
[4] P.P. Pelligrini, J.R. Aldrich-Wright, Dalton Trans. (2003) 176–183.
[5] P.U. Maheswari, M. Palaniandavar, Inorg. Chim. Acta 357 (2004) 901–912.
[6] F. Gao, H. Chao, F. Zhou, Y.X. Yuan, B. Peng, L.N. Ji, J. Inorg. Biochem. 100 (2006) 1487–1494.
[7] L.F. Tan, X.H. Liu, H. Chao, L.N. Ji, J. Inorg. Biochem. 101 (2007) 56–63.
[8] B. Norden, P. Lincoln, B. Akerman, E. Tuite, Met. Ions. Biol. Syst. 33 (1996) 177–252.
[9] K.E. Erkkila, D.T. Odom, J.K. Barton, Chem. Rev. 99 (1999) 2777–2796.
[10] C. Metcalfe, J.A. Thomas, Chem. Soc. Rev. 32 (2003) 215–224.
[11] H.J. Shi, Y. Chen, F. Gao, H.J. Yu, G.Y. Li, H. Chao, X.F. Shi, L.N. Ji, J. Mol. Struc. 892 (2008) 485–489.
[12] X.W. Liu, L.C. Xu, H. Li, H. Chao, K.C. Zheng, L.N. Ji, J. Mol. Struc. 920 (2009) 163–171.
[13] H.J. Yu, S.M. Huang, L.Y. Li, H.N. Ji, H. Chao, Z.W. Mao, J.Z. Liu, L.N. Ji, J. Inorg. Biochem. 103 (2009) 881–890.
[14] L.F. Tan, X.L. Liang, X.H. Liu, J. Inorg. Biochem. 103 (2009) 441–447.
[15] D.L. Arochiasamy, S. Radhika, R. Parthasathi, B.N. Nair, Eur. J. Med. Chem. 44 (2009) 2044–2051.
[16] P.J. Dandliker, R.E. Holmline, J.K. Barton, Science 275 (1997) 1465–1468.
[17] X.J. Yang, C. Janiak, J. Heinze, F. Drepper, P. Meyer, H. Piotrowski, P. Klufers, Inorg. Chim. Acta 318 (2001) 103–116.
[18] J. Liu, W.J. Zheng, S. Shi, C.P. Tan, J.C. Chen, K.C. Zheng, L.N. Ji, J. Inorg. Biochem. 102 (2008) 193–202.
[19] C.P. Tan, J. Liu, L.M. Chen, S. Shi, L.N. Ji, J. Inorg. Biochem. 102 (2008) 347–358.
[20] E.A. Steck, A.R. Day, J. Am. Chem. Soc. 65 (1943) 452–456.
[21] B.P. Sullivan, D.J. Salmon, T.J. Meyer, Inorg. Chem. 17 (1978) 3334–3341.
[22] Y.J. Liu, C.H. Zeng, H.L. Huang, L.X. He, F.H. Wu, Eur. J. Med. Chem. 45 (2010) 564–571.
[23] Y.J. Liu, C.H. Zeng, F.H. Wu, J.H. Yao, L.X. He, H.L. Huang, J. Mol. Struc. 932 (2009) 105–111.
[24] Y.J. Liu, X.Y. Wei, F.H. Wu, W.J. Mei, L.X. He, Spectrochim. Acta Part A 70 (2008) 171–176.
[25] S. Shi, J. Liu, J. Li, K.C. Zheng, C.P. Tan, L.M. Chen, L.N. Ji, J. Chem. Soc, Dalton Trans. (2005) 2038–2046.
[26] J.Z. Wu, B.H. Ye, L. Wang, L.N. Ji, J.Y. Zhou, R.H. Li, Z.Y. Zhou, J. Chem. Soc, Dalton Trans. (1997) 1395–1401.
[27] J.G. Liu, B.H. Ye, H. Li, Q.X. Zhen, L.N. Ji, Y.H. Fu, J. Inorg. Biochem. 76 (1999) 265–271.
[28] A.E. Friedman, J.C. Chambron, J.P. Sauvage, N.J. Turro, J.K. Barton, J. Am. Chem. Soc. 112 (1990) 4960–4962.
[29] S. Satyanarayana, J.C. Dabrowiak, J.B. Chaires, Biochemistry 32 (1993) 2573–2584.
[30] M.J. Waring, J. Mol. Biol. 13 (1965) 269–274.
[31] G.A. Neyhart, N. Grover, S.R. Smith, W.A. Kalsbeck, T.A. Fairly, M. Cory, H.H. Thorp, J. Am. Chem. Soc. 115 (1993) 4423–4428.
[32] J.D. McGee, Biopolymers 15 (1976) 1345–1375.
[33] M.T. Carter, M. Rodriguez, A. Bard, J. Am. Chem. Soc. 111 (1989) 8901–8911.
[34] H.Q. Liu, B.C. Tzeng, Y.S. You, S.M. Peng, H.L. Chen, M.S. Yang, C.M. Che, Inorg. Chem. 41 (2002) 3161–3171.
[35] J.K. Barton, A.L. Raphael, J. Am. Chem. Soc. 106 (1984) 2466–2468.
[36] C.C. Cheng, S.E. Rokita, C.J. Burrows, Angew. Chem. Int. Ed. Engl. 32 (1993) 277–278.
[37] S.A. Lesko, R.J. Lorentzen, P.O. Ts'o, Biochemistry 19 (1980) 3023–3028.
[38] R. Nilsson, P.B. Merkel, D.R. Kearns, Photochem. Photobiol. 16 (1972) 117–124.
[39] H.L. Huang, G.P. Tang, Q.Q. Wang, D. Li, F.P. Shen, J. Zhou, H. Yu, Chem. Commun. (2006) 2382–2384.
[40] V. Vijayanathan, T. Thomas, A. Shirahata, T.J. Thomas, Biochemistry 40 (2001) 13644–13651.
[41] T. Sarkar, A.S. Petrov, J.R. Vitko, C.T. Santai, S.C. Harvey, I. Mukerji, N.V. Hud, Biochemistry 48 (2009) 667–675.
[42] B. Sun, J.X. Guan, L. Xu, B.L. Yu, L. Jiang, J.F. Kou, L. Wang, X.D. Ding, H. Chao, L. N. Ji, Inorg. Chem. 48 (2009) 4637–4639.
[43] U. Schatzschneider, J. Niesel, I. Ott, R. Gust, H. Alborzinia, S. Wölfl, ChemMedChem 3 (2008) 1104–1109.
[44] M. Harlos, I. Ott, R. Gust, H. Alborzinia, S. Wölfl, A. Kromm, W.S. Sheldrick, J. Med. Chem. 51 (2008) 3924–3933.
[45] J.A. Hickman, Cancer Metastasis Rev. 11 (1992) 121–139.
[46] T.R. Li, Z.Y. Yang, B.D. Wang, D.D. Qin, Eur. J. Med. Chem. 43 (2008) 1688–1695.
[47] J. Marmur, J. Mol. Biol. 3 (1961) 208–211.
[48] M.E. Reichmann, S.A. Rice, C.A. Thomas, P. Doty, J. Am. Chem. Soc. 76 (1954) 3047–3053.
[49] J.B. Chaires, N. Dattagupta, D.M. Crothers, Biochemistry 21 (1982) 3933–3940.
[50] S. Satyanaryana, J.C. Dabrowial, J.B. Chaires, Biochemistry 31 (1992) 9319–9324.
[51] G. Cohen, H. Eisenberg, Biopolymers 8 (1969) 45–49.
[52] T. Mosmann, J. Immunol. Methods 65 (1983) 55–63.
[53] D.L. Spector, R.D. Goldman, L.A. Leinwand, In Cells: A Laboratory Manual, vol. 1, Cold Spring Harbor Laboratory Press, New York, 1998, Chapter 15.